journal

J. Am. Ceram. Soc., 77 [9] 2337–44 (1994)

Temperature–Time Texture Transition of $Pb(Zr_{1-x}Ti_x)O_3$ Thin Films: II, Heat Treatment and Compositional Effects

San-Yuan Chen* and I-Wei Chen*

Department of Materials Science and Engineering, University of Michigan, Ann Arbor, Michigan 48109-2136

Texture transition of $Pb(Zr_{1-x}Ti_x)O_3$ thin films grown from a metallo-organic solution onto $Pt/Ti/SiO_2/Si$ substrates has been studied. The orientation obtained depends on the crystallization temperature and time and can be drastically altered by modifying the heat treatment schedule. A [100] texture requires an initial seeding treatment in the intermediate temperature range. This is attributed to a nucleation advantage associated with the formation of an intermediate PbO[001] texture that tends to form at intermediate temperature over time. A [111] texture develops at higher temperature during rapid heating and can be rationalized by the formation of an epitaxial intermetallic phase $Pt_{5-7}Pb$ at the PZT/Pt interface that provides lattice matching between PZT(111), $Pt_{5-7}Pb(111)$, and Pt(111). Temperature–time transformation texture (TTT) diagrams of PZT texture have been constructed for seeding various orientations. The effect of composition (Pb excess and Zr/Ti ratio) and the possible manipulation of these texture selection relations by combining compositional tailoring and heat treatment schedules are illustrated.

I. Introduction

THE selection of a preferred orientation in $Pb(Zr_{1-x}Ti_x)O_3$ (PZT) films is usually based on the substrate used. For example, PZT films with [100], [110], and [111] textures can be obtained by using single-crystal $SrTiO_3$ wafers of the same orientations.[1] Likewise, when a sol–gel-derived film forms on a $Pt(111)/Ti/SiO_2/Si$ substrate, [111] texture has been reported,[2] whereas [100]/[001] textures are obtained on Pt(100)/MgO(100).[3,4] More recently, it has been realized that more than one texture can be obtained on the same substrate if different processing conditions are used. For example, highly textured [100] and [111] films pyrolyzed from sol–gel or metallo-organic solutions have been reported on a $Pt(111)/Ti/SiO_2/Si$ substrate.[5–6] Understanding the processing conditions that lead to these texture selections offers better control and optimization of the structure and properties of the PZT films.

To identify the mechanisms of texture selection of PZT films on the Pb(111) substrate, we performed experiments to isolate the critical intermediate phases formed at the substrate surface that seed the oriented crystal.[7,8] A layer of intermetallic phase $Pt_{5-7}Pb$ was found at the PZT/Pt interface.[7] This intermetallic phase is epitaxial with Pt and provides a well-matched buffer for the lattice relationship of $PZT(111)/Pt_{5-7}Pb(111)/Pt(111)$. The condition for forming $Pt_{5-7}Pb$ requires a locally reducing atmosphere which is favored at the buried substrate/film interface during the early stage of pyrolysis. Later, when oxygen is replenished by the air intake, the intermetallic is reoxidized. Experimentally, rapid heating to high temperature seems to lead consistently to the formation of $Pt_{5-7}Pb$.[7]

We also found that the [100] texture on Pt(111) is correlated with the formation of a PbO(001) layer.[6] The PbO is textured because of the nature of the layer compound, which can be further attributed to Pb that has lone-pair electrons. The PbO(001) plane had reasonably good matching with PZT(100), which facilitated the selection of the texture. The formation of PbO is possible under very general conditions other than the one that favors $Pt_{5-7}Pb$. Experimentally, this can be consistently obtained by heating at intermediate temperatures.[8]

Based on the above information, we systematically performed different heat treatments to document the formation conditions of different PZT textures. Also investigated were the compositional effects. To better define the correspondence between the texture and the kinetic pathway, we developed a set of temperature–time transformation texture diagrams in analogy to the conventional TTT diagram that describes the structure–processing relation for diffusive phase transformation. These results are reported here and interpreted using the knowledge of intermediate phases.

II. Experimental Procedures

(1) *Preparation of Stock Solution*

A metallo-organic decomposition (MOD) process was used in this study. The precursor solutions used to prepare $Pb(Zr_{1-x}Ti_x)O_3$ were lead 2-ethylhexanoate ($Pb(C_8H_{15}O_2)_2$), zirconium octoate ($Zr(C_7H_{15}COO)_4$), both obtained from a commercial source, and titanium-diethoxydineodecanoate ($Ti(OC_2H_5)_2(C_9H_{19}COO)_2$) which was synthesized in our laboratory. The procedure used to fabricate these precursor solutions was previously described in detail.[9] The metallic cations in the above liquid solution are fully coordinated to organic functional groups, but are otherwise physically and chemically separated from each other and distributed randomly. This contrasts with a typical sol–gel solution in which two or more metallic cations are incorporated into a polymeric network, sometimes in a preferential manner that favors association of certain cation pairs. Since such a preferential cation association is known to profoundly influence the subsequent reaction pathway for lead-based ferroelectrics,[10] the metallo-organic decomposition method offers a more straightforward physical/chemical route from solution to oxide and is quite suitable for the purpose of elucidating the kinetics and mechanisms of orientation selection.

(2) *Fabrication of Thin Films*

Thin films were fabricated on $Pt(111)/Ti/SiO_2/Si$ substrates by spin coating. (The Ti layer between Pt and SiO_2 was present to improve Pt adhesion.) Before use, the Pb(111)-coated Si substrates were boiled in deionized water and then in 2-propanol for 5 min. After full pyrolysis, a single-layer, crack-free film ranging from 0.1- to 0.3-μm thickness was fabricated. Many heating schedules have been used and all of them include a low-temperature drying step at 150°C, for 0.5 h, to drive off the solvent. The subsequent heating schedules vary and some include

S.-I. Hirano—contributing editor

Manuscript No. 193951. Received December 21, 1993; approved May 27, 1994.
Supported by the U.S. Department of Energy (BES) under Grant No. DE-FG02-87ER45302.
*Member, American Ceramic Society.

an intermediate pyrolysis step, say at 450°C for 0.5 h. The final heat treatment is typically at 700°C for 0.5 h. Fast heating was also conducted by placing a dried film directly into a furnace at a preset temperature for various times and then fast cooling. Specific variations of heating schedules will be described in the Results and Discussion section.

(3) Characterization of Solutions and Thin Films

Thermal analysis of solutions using TGA and DTA was performed to identify the major evaporation, decomposition, and phase crystallization steps during pyrolysis. The orientation of the film was determined by the standard θ–2θ X-ray diffraction (XRD) method. In addition, since (111) reflections of Pt and $PbTiO_3$ are rather close to each other, a Seemann–Bohlin diffractometer, which can suppress the (Pt) substrate reflection, was used to verify the observed PZT texture in Ti-rich PZT compositions. The integrated intensities of three perovskite peaks, (100), (110), and (111), were used to quantify texture. This was deemed adequate, since our aim was to compare textures of samples in our process, where all diffraction conditions are constant. These peak intensities were normalized by the corresponding intensities obtained for randomly oriented powder samples. The relative intensity then is defined as

$$(I/I^*)/[(I/I^*)_{100} + (I/I^*)_{110} + (I/I^*)_{111}]$$

where I represents the integrated intensity of a particular reflection (100, 110, or 111) for the film and I^* represents its counterpart for the powdered sample. In this way, the influence of the different scattering functions of different reflections is removed from the texture represented. (For a more rigorous quantitative analysis, orientation distribution functions must be obtained from pole figure measurements. This was not attempted in our work.) For the (111) peak that falls on the broad shoulder of Pt(111), a deconvolution procedure was included in this analysis. Finally, microstructure and thickness of films were examined using scanning electron microscopy (SEM).

III. Results and Discussion

(1) Thermal Analysis of Precursor Solutions

Figure 1 shows the DTA–TGA curves of the mixture solution of lead 2-ethylhexanoate, titanium diethoxy-dineodecanoate, and zirconium octoate from room temperature to 800°C obtained at a heating rate of 5°C/min. The TGA curve shows a major weight loss below 150°C due to the evaporation of low-boiling-point solvents (xylene and mineral spirits). The weight loss between 150° and 370°C corresponds to removal and decomposition of organic groups such as octoate, 2-ethylhexanoate, and neodecanoate. After that, no apparent weight loss could be detected and the pyrolysis was considered complete. Regarding the DTA curve, the endothermic peak at about 100°C corresponds to the evaporation of solvents. The two exothermic peaks at 320° and 350°C result from PbO formation[8] and progressive decomposition of organic compounds. Two other broad exothermic peaks that are associated with crystallization can also be identified in the DTA curve. One starts around 370°C, when pyrochlore is formed, and the other begins at about 480°C, when perovskite is formed.

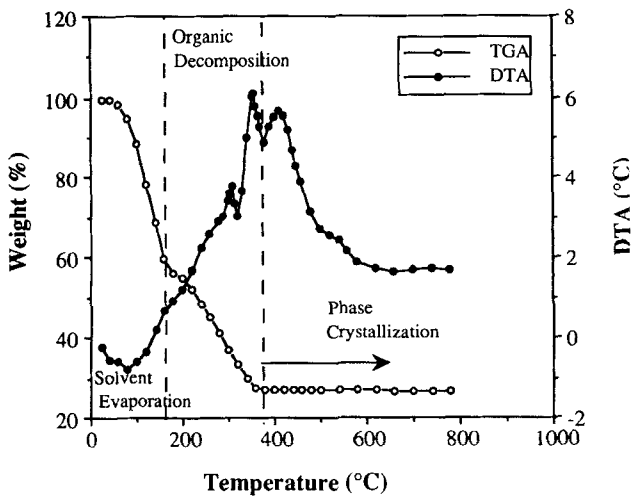

Fig. 1. DTA and TGA curves of PZT precursor solution in air with a heating rate of 5°C/min.

It should be noted that the above temperatures are upper bounds, since phase formation in small amounts and in small crystallite sizes would give too weak a signal to be detected by DTA and XRD. On the other hand, crystallization of thin film usually proves somewhat more difficult and requires higher temperature, possibly because of constraining interfacial stresses which developed during unidirectional shrinkage.[11] The film is generally amorphous below 350°C and probably remains largely so up to 450°C for a pyrolyzing time of 0.5 h. The maximum amount of pyrochlore was detected around 500°C.

(2) Phase Evolution during Isothermal Annealing

Isothermal annealing of dried films was performed by placing the films in a furnace with a preset temperature and then rapidly withdrawing the samples after a set time. At the lower annealing temperature, e.g., 500°C, the intermetallic phase $Pt_{5-7}Pb$ was found around 3–5 min (Fig. 2(a)). This phase disappears after 10 min, and a broad peak around 29° 2θ, identified as microcrystalline pyrochlore phase, appears, which later gives way to perovskite after 2 h. This perovskite has a strong [100] texture, as shown in Fig. 2(a). The same evolution is seen also at 550°C but it proceeds much faster. Below 485°C, no perovskite peak can be seen even after 20 h.

At the higher annealing temperature, e.g., 625°C, the epitaxial $Pt_{5-7}Pb$ phase formed after a very short time (1–2 min). It disappeared after 4 min when PZT(111) began to form. The phase evolution is shown in Fig. 2(b). (Note that the intensity scales in Fig. 2 are not the same for different scans, so the relative intensities should refer to the Pt(111) peak.) The peak positions for $Pt_{5-7}Pb(111)$, 38.5°, and PZT(111), 38.1°, are very close.

The above results can be interpreted using the model presented in our previous paper[7] as follows. At a lower temperature, e.g., 500°C, the perovskite formation is very slow. Thus, although $Pt_{5-7}Pb$ phase formed first, it subsequently oxidizes and decomposes without nucleating PZT[111] texture. After longer annealing, the PbO(001) layer forms on the substrate on which PZT(100) eventually forms. At a higher temperature, e.g., 625°C, the perovskite forms rapidly. Since the first phase obtained is always $Pt_{5-7}Pb(111)$, the PZT(111) forms onto this phase and dominates the texture. The $Pt_{5-7}Pb$ later decomposes after a few minutes but leaves the PZT[111] texture intact.

The normalized relative intensity for three perovskite reflections as a function of annealing temperature (holding time is 1 h) is shown in Fig. 3. Other observations worth noting are (a) the pyrochlore-to-perovskite transformation is essentially complete above 550°C; (b) the pyrochlore phase formed below 550°C is probably not textured and is not related to the PZT texture;[8] (c) the perovskite is always highly textured (in the randomly oriented powder sample, (110) is the strongest peak); (d) as temperature increases, [111] texture is favored over [100] texture; (e) only [111] texture forms and levels off for temperatures over 600°C; and (f) the perovskite is stable up to 800°C, above which PbO rapidly evaporates and a Pb-deficient pyrochlore-type phase of $PbTi_3O_7$ phase begins to appear. This pyrochlore phase has been reported by others for films held at 775°C for 1 h.[12]

(3) Texture Selection and Thermal History

The above result seems to indicate that a [100] texture is unstable at higher temperatures. However, we have found that the [100] texture for perovskite can be preserved at about

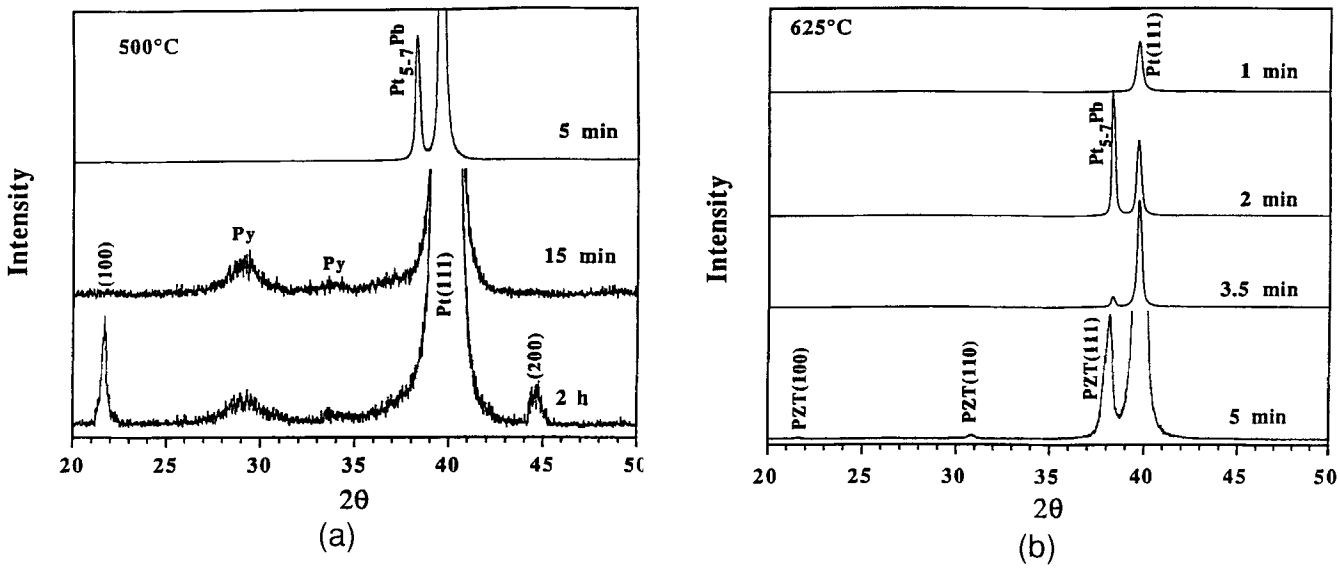

Fig. 2. XRD patterns of PZT films heated for different times at (a) 500°C and (b) 625°C.

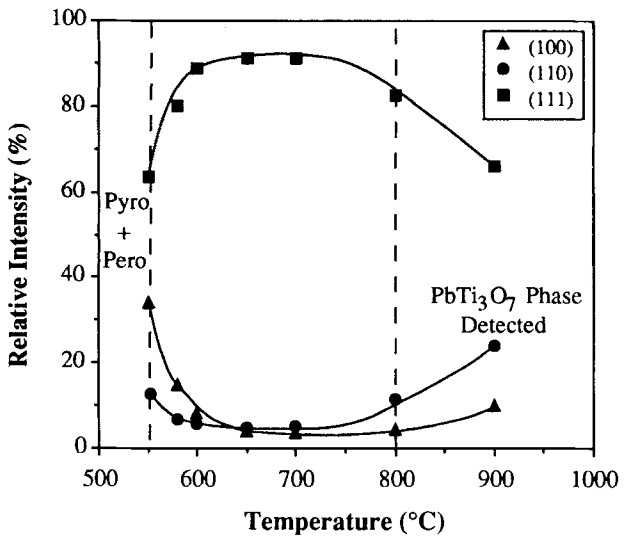

Fig. 3. Normalized relative intensity for three perovskite reflections as a function of annealing temperature (1 h).

600°C, using a different heat treatment. For example, if the film is first held at 450°C for 0.5 h, cooled, then rapidly heated to 700°C and held for 0.5 h, a very strong [100] texture is obtained (Fig. 4(a)). The important point to note is that, after 450°C treatment, no trace of perovskite is detectable by XRD—only a pyrochlore phase is present. Thus, crystallization, pyrochlore-to-perovskite transformation, and the growth of [100] texture are all achieved at 700°C in the above procedure. If the 450°C treatment is replaced by pyrolysis at 350°C, followed by fast heating to 700°C, then a [111] texture is observed instead (Fig. 4(b)). In this case, after 350°C pyrolysis for 0.5 h, the film is still mostly amorphous. Likewise, if the films were directly heated to 700°C without any pyrolysis, the [111] texture still dominates. Therefore, the texture obtained in 700°C crystallization is strongly dependent on the previous thermal history at lower temperatures. In fact, we can even obtain a film of an apparently random texture almost indistinguishable from that of the powdered sample (Fig. 4(c)) by very slow heating (1°C/min) from 150° to 700°C.

Clearly, the texture transition is not thermodynamic but rather dependent on the kinetic pathway. The above results can be interpreted in the following way. During the isothermal hold at 450°C, the time (0.5 h) is sufficiently long to decompose $Pt_{5-7}Pb$ and to grow PbO(001), with possibly some PZT (100) microcrystallites also forming on PbO, but its quantity is too small to be detected. It later grows at 700°C when the kinetics are much faster. If the isothermal hold is below 350°C, however, the temperature is too low even for $Pt_{5-7}Pb$ or PbO formation. (The lowest formation temperatures for these phases were found around 370°C.) Thus, no effect on texture is imprinted by this heat treatment, and the texture is entirely determined by the fast heating treatment to 700°C that favors $Pt_{5-7}Pb$ and PZT[111]. Lastly, during slow heating, PZT formation is possible over a wide range of temperatures and times. Although [100] texture might have been expected to dominate, we found that the PbO[001] texture on the Pt(111) substrate was actually unstable after long annealing. (In the literature it has been reported that PbO starts to evaporate at the temperature range 450°–550°C in the $(Pb,La)TiO_3$ films.[13]) Thus, both [111] and [100] textures are eliminated, which allows other variants to nucleate and grow on the substrate, resulting in a mixture of both [100] and random textures ((110) being the strongest reflection).

The effect of the heating rate is shown in Fig. 5 for the relative XRD intensity of specimens heated from room temperature to 700°C. The random [100] texture and [111] texture become dominant at progressively higher heating rates. These results are consistent with the interpretation above and require no further discussion.

(4) TTT Curves

To more precisely identify the correspondence between kinetic pathway and texture, we performed a set of experiments in which the "growth kinetics" were kept the same but the "nucleation kinetics" were varied. This was motivated by the thinking that initial crystallization at the pyrolyzing temperature could dictate the orientation of perovskite "seed" crystals which are inherited in the subsequent development. These seed crystals could be very small and of a very minute amount, thus below the detection limit of XRD. Therefore, to evaluate the success of seeding reactions, we grew the film at a higher temperature for a set time to allow the development of the texture from the seeds. From these results, a temperature–time transformation texture (TTT) diagram which is conceptually similar to the temperature–time transformation diagram in the literature of diffusive phase transformation[14] can be constructed from the heat treatment conditions (temperature and time) used for the seeding. In practice, the seeding treatment was performed by rapidly heating the samples to the seeding temperatures and

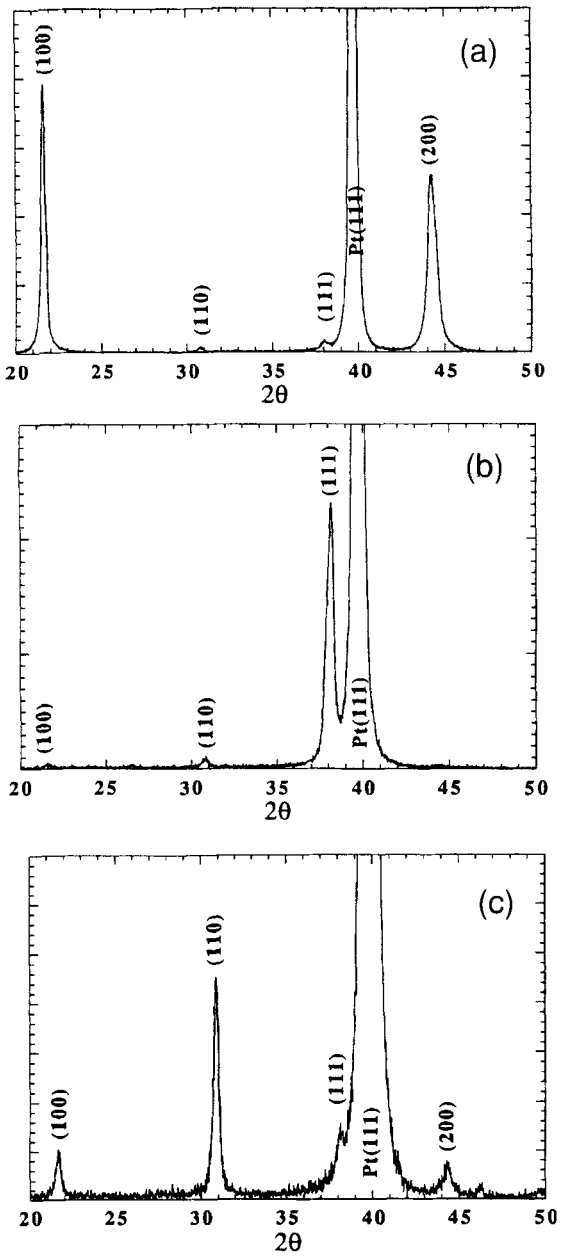

Fig. 4. XRD patterns of three PZT samples: (a) [100] texture pyrolyzed at 450°C and annealed at 700°C, (b) [111] texture fast heated to 700°C, and (c) random texture slowly heated to 700°C.

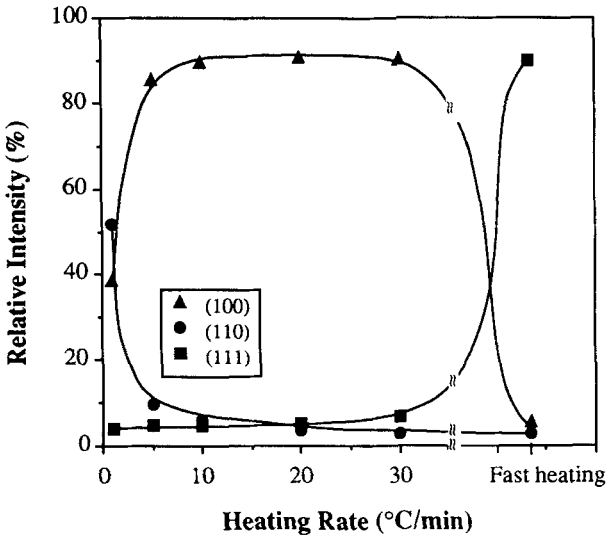

Fig. 5. Normalized relative intensity for three perovskite reflections as a function of heating rate to 700°C.

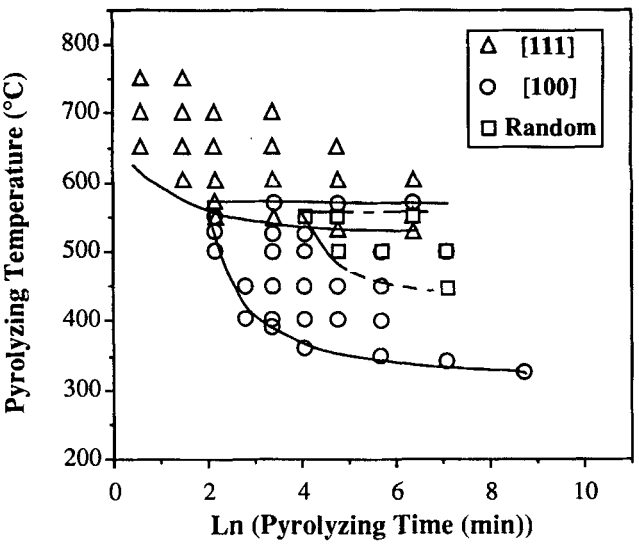

Fig. 6. TTT diagram for seeding texture in PZT film on Pt(111) substrate.

holding for various times, then rapidly cooling them. For the growth treatment, the seeded samples were rapidly heated to 700°C and annealed for 0.5 h to effect crystallization and pyrochlore-to-perovskite transformation. The observed textures after the growth treatment are mapped in Fig. 6 in a semilogarithm plot of seeding temperature against seeding time.

In principle, we expect a TTT diagram to consist of three C-shaped curves, representing the seeding of [100], [111], and random textures. However, for the [111] regime, the upper boundary is not shown in Fig. 6, because the temperature would be so high as to cause PbO evaporation and $PbTi_3O_7$ formation. The upper boundary of the (100) regime is essentially flat, and intersects the regime of [111] from 570° to 530°C. The random regime, which is entered when the sample is pyrolyzed for a long time ($t > 2$ h) in the temperature range of 450° to 550°C, resembles the classical C-shape the best. The unmarked region to the left of the [111] and [100] boundaries in Fig. 6 represents pyrolyzing conditions insufficient for crystallization. In this regime, the sample is still amorphous, and during later heating at 700°C it forms PZT[111] texture just the same as unpyrolyzed samples that are directly heated to 700°C.

Using the TTT diagram, the texture correspondence to thermal history can be fully explained. For example, referring to Fig. 4(a), heat treatment at 450°C for 0.5 h is seen to complete [100] seeding, which becomes fully developed during later crystallization. Referring to Fig. 4(b), pyrolysis at 350°C for 0.5 h is seen to be too short for [100] seeding, and the film is mostly amorphous. Thus, subsequent crystallization at 700°C is dominated by [111] texture. Lastly, referring to Fig. 4(c), slow heating is seen to traverse through [100], random, and [111] regimes, in that order. This multiple seeding sequence results in a random texture.

The above TTT diagram is again shown in Fig. 7, in which the formation region of $Pt_{5-7}Pb$ reported in our previous work is outlined.[7] Also shown in the shaded area is the starting temperature/time observed for PbO formation in simulation experiments, when PbO composition is used. These results are consistent with the concept that the transformation temperature of pyrochlore to perovskite is 550°C, that above this temperature $Pt_{5-7}Pb$ can directly nucleate PZT[111] (Fig. 3), and that below this temperature $Pt_{5-7}Pb$ oxidizes to form PbO(001)

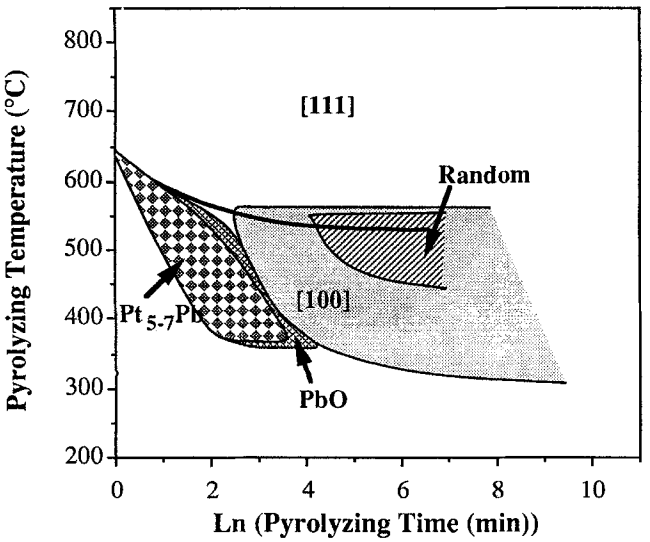

Fig. 7. TTT diagram (as in Fig. 6) with the formation regions of $Pt_{5-7}Pb$ and PbO phases.

which in turn can nucleate PZT[100]. Also note that, after long annealing, PbO(001) begins to evaporate and partially gives way to PbO in other orientations, causing the PZT random region to emerge. Mixtures of textures can also be observed in the borderline cases. They can all be understood in terms of PZT seeding on $Pt_{5-7}Pb(111)$ and/or PbO(001).

(5) Pb Composition

Nominal compositions of $Pb_{1+x}(Zr_{0.52}Ti_{0.48})O_{3+x}$ (where $x = -0.1$ to 0.15) were prepared to investigate the effect of excess/deficient Pb. These films were given two heat treatments which would favor PZT[111] and PZT[100] textures, respectively. In the first case, fast heating to 700°C (hold time = 0.5 h) was used. In the second case, pyrolysis at 450°C for 0.5 h, then fast heating to 700°C (hold time = 0.5 h), was used. As shown in Fig. 8(a), the PZT[111] texture dominates after the first heat treatment is nearly independent of Pb composition. This compares with the PZT[100] texture, which dominates after the second heat treatment but is more favored by an excess Pb composition. Referring to the seeding requirement, these results may suggest that the formation of $Pt_{5-7}Pb$ is always favored; however, the formation of PbO requires Pb excess. This is reasonable, because the driving force for the formation of $Pt_{5-7}Pb$ comes from the locally reducing atmosphere generated by pyrolysis, causing the least refractory element Pb to be reduced. Thus, Pb excess is not essential for the process. On the other hand, the driving force for PbO formation obviously decreases as the amount of Pb excess is reduced, and the above results are thus consistent with our interpretation of the formation mechanisms.

A review of the literature found a similar correlation between excess PbO composition and PZT[100] texture. Iijima *et al.*[15] reported that PbO-rich targets are necessary to obtain *c*-axis-oriented $PbTiO_3$ films on (100) MgO single-crystal substrate using RF-magnetron sputtering. PZT with [100] texture can also be made in a similar way.[16] Recently, both [111] and [100] textured films of (Pb,La)TiO_3 on (0001) Al_2O_3 sapphire were obtained using multi-ion-beam reactive cosputtering.[17] Xiao *et al.* reported that [111] texture readily formed under routine sputtering conditions, but [100] texture formed only when the incident energy of ions for sputtering Pb target was increased, i.e., in a Pb-rich condition. These results are consistent with our finding that the Pb-rich intermediate layer between PZT and Pt promotes a [100] texture.

(6) Zr/Ti Composition

PZT compositions of $Pb(Zr_{1-x}Ti_x)O_3$ with $x = 0$ to 1 were prepared to investigate the effect of the Zr/Ti ratio. At high temperatures, when PZT perovskite forms, only the cubic phase is stable throughout the entire range of composition. Thus, the different phases seen in this system at room temperature are not of concern for texture seeding and growth mechanism. On the other hand, since the lattice constant decreases systematically from $PbZrO_3$ to $PbTiO_3$, with $PbTiO_3(111)$ matching $Pt_{5-7}Pb(111)$ better than $PbZrO_3$, we do expect a compositional effect on [111] texture selection. (For $PbZrO_3$, (240) peak corresponds to PZT(111) and $PbTiO_3(111)$. It is indexed differently because of different unit cells.) This expectation was borne out in our study using the first heat treatment described in the previous section. We found that, after rapid annealing at 700°C, only $PbTiO_3$ develops a strong [111] texture, whereas texturing in $PbZrO_3$ is preferentially [120] and [100] as evidenced by relatively strong (240) and (200) diffraction peaks, respectively (they correspond to [111] and [100] textures in PZT). The results are shown in Fig. 9(a). Shown in Fig. 9(b) is the strong [100] texture for both $PbTiO_3$ and $PbZrO_3$ using the second heat treatment described in the previous section.

The relative intensity of different orientations is shown as a function of composition in Figs. 10(a) and (b) for the two heat

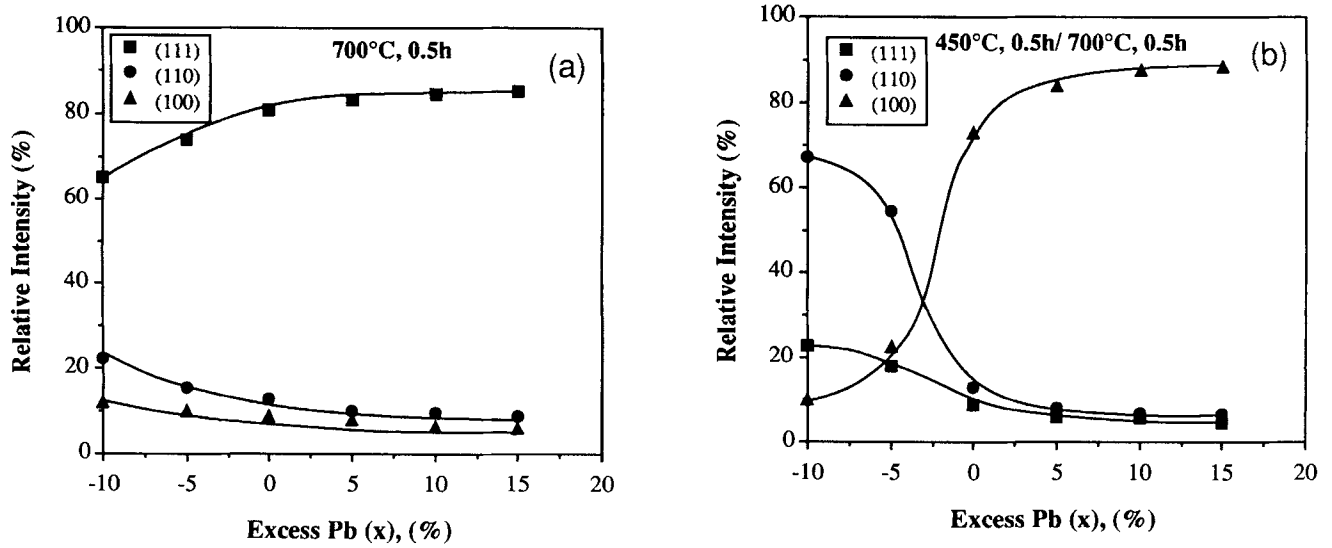

Fig. 8. Effect of excess Pb (x) in $Pb_{1+x}(Zr_{0.52}Ti_{0.48})O_{3+x}$ on relative intensity of PZT films for (a) fast heated to 700°C and (b) pyrolyzed at 450°C (0.5 h) and annealed at 700°C.

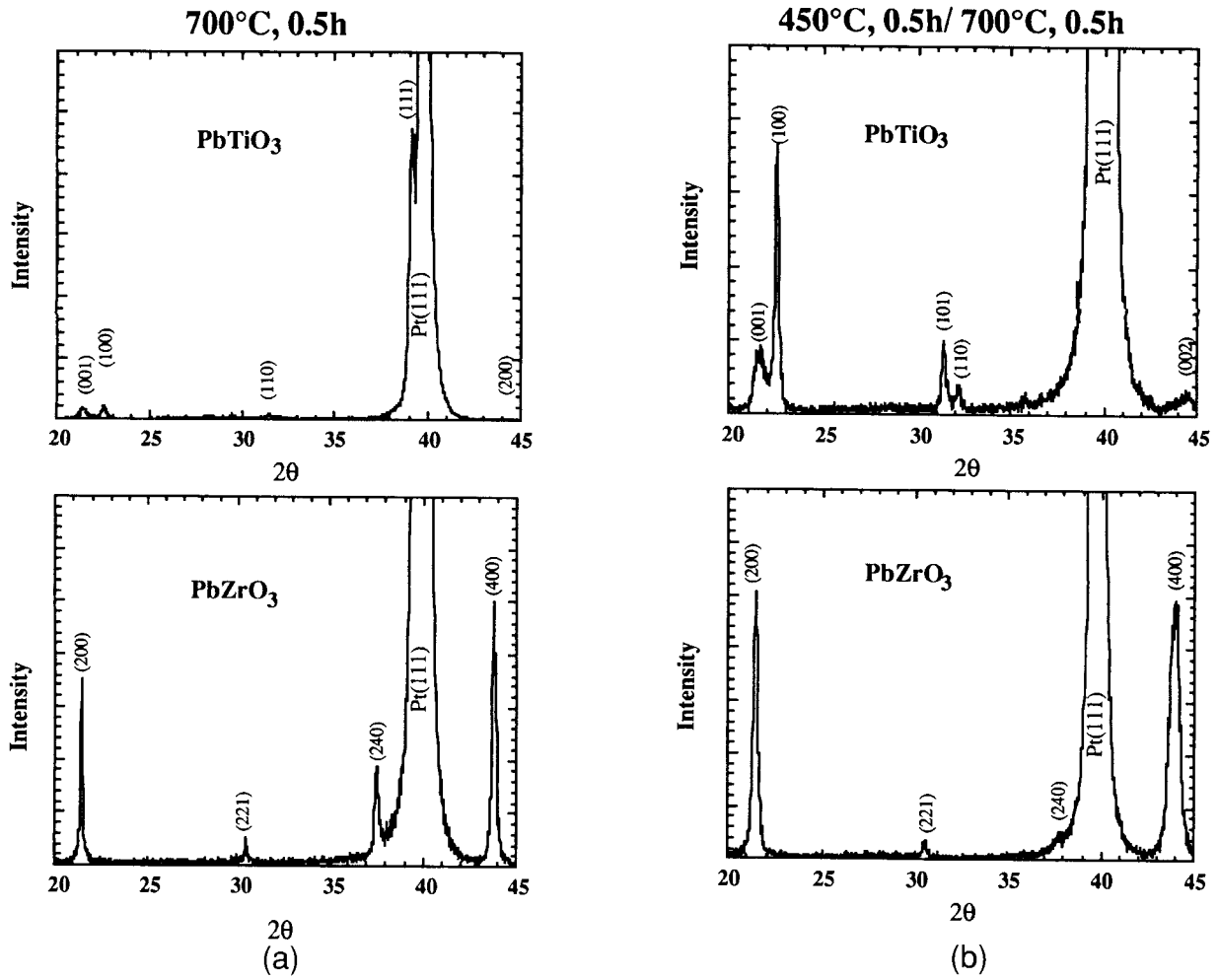

Fig. 9. XRD patterns of $PbTiO_3$ and $PbZrO_3$ films for (a) fast heated to 700°C and (b) pyrolyzed at 450°C (0.5 h) and annealed at 700°C.

treatments. Figure 10(a) shows that [111] orientation is preferred for Ti-rich PZT compositions, consistent with the expectation of a poor [111] texture for the Zr-rich compositions because of a poor lattice match. (The slight decrease in relative intensity of (111) peak for $PbTiO_3$ is possibly due to the cubic-to-tetragonal transformation in this compound that alters the multiplicity and scattering factors, although the decrease is small enough to be due to other considerations affecting diffraction of highly oriented films.) On the other hand, Fig. 10(b) shows that the [100] texture seems to dominate the whole composition range. This suggests that the formation of PbO(001) layer is always favored. The lower (100) intensity at the Ti-rich end is believed to imply a weaker tendency for forming PbO(001). This tendency is consistent with the higher affinity of PbO to TiO_2 than to ZrO_2, as supported by the data of PbO vapor pressure which decreases as a function of x in the $Pb(Zr_{1-x}Ti_x)O_3$ system.[18]

A related aspect is the dependence of crystallization temperature of the perovskite phase on the Zr/Ti composition and the attendant effect on microstructure. By XRD and DTA, we found that perovskite formation is more difficult in $PbZrO_3$ (above 600°C) than in $PbTiO_3$ (above 500°C), for the same pyrolysis treatment of 0.5 h. This compares with the formation temperature in $Pb(Zr_{0.52}Ti_{0.48})O_3$, which is 550°C. The difficulty in perovskite crystallization is in turn reflected in the larger grain size seen in the Zr-rich films. As shown in Fig. 11, the grain size increases in the order of $PbTiO_3$, $Pb(Zr_{0.52}Ti_{0.48})O_3$, and $PbZrO_3$ for both sets of heat treatment. This is attributed to the smaller number of perovskite nuclei in the Zr-rich composition which crystallizes with more difficulty.

(7) Seeding Effect

Our model for the texture formation mechanisms implies that once a texture is produced in the first layer, the same texture should prevail in subsequent growth regardless of heating schedule and composition used for the outer layer. If so, a seeding heat treatment or a special composition can be used to promote the texture formation in cases where the desired texture is difficult to obtain under normal circumstances. For example, we obtained a [111] texture for Zr-rich PZT films (i.e., [240] texture in $PbZrO_3$) by first depositing a PZT[111] layer. This is shown in Fig. 12(a) which provides both the microstructure and the XRD pattern. The seeding layer was $Pb(Zr_{0.52}Ti_{0.48})O_3$ and was fast heated to 700°C for 0.5 h, producing a [111] orientation. The second layer was $Pb(Zr_{0.75}Ti_{0.25})O_3$ (fast heated to 700°C) which inherited the [111] texture from the first layer. (Note that without the first seeding layer, the $Pb(Zr_{0.75}Ti_{0.25})O_3$ composition would have yielded a mixed [100]/[111] texture according to Fig. 10(a).) For comparison, Fig. 12(b) shows the microstructure and XRD of a two-layer film with the inner layer being $Pb(Zr_{0.52}Ti_{0.48})O_3$ [111] and the outer layer being $Pb(Zr_{0.25}Ti_{0.75})O_3$ [111], heat treated in the same way as above. Comparing Figs. 12(a) and (b), we find a similar texture and grain size in both compositions with the same seeding first layer. This contrasts with the much weaker [111] texture and much larger grain size for the Zr-rich composition when fast fired to 700°C without the first seeding layer (see Figs. 10(a), 11(d), and 11(f)). Thus, crystallization of the perovskite phase is apparently easier with the presence of a perovskite seeding layer which is now seen to control the microstructure of the subsequent perovskite layers in addition to controlling the texture.

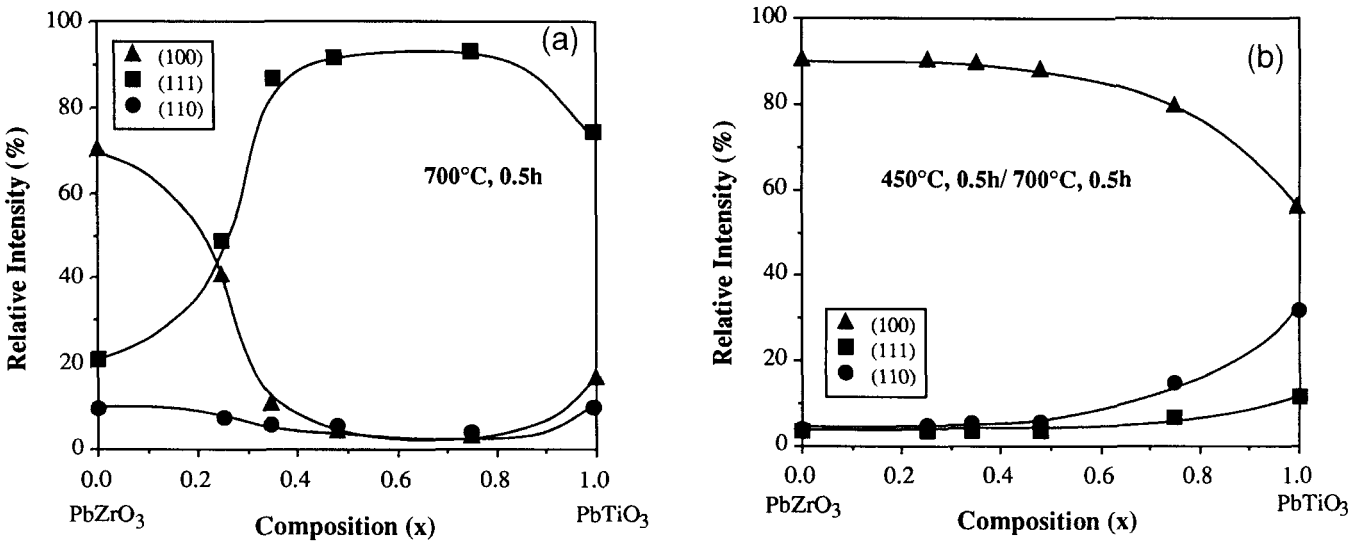

Fig. 10. Effect of Zr/Ti composition (x) in $Pb(Zr_{1-x}Ti_x)O_3$ on relative intensity of PZT films for (a) fast heated to 700°C and (b) pyrolyzed at 450°C (0.5 h) and annealed at 700°C.

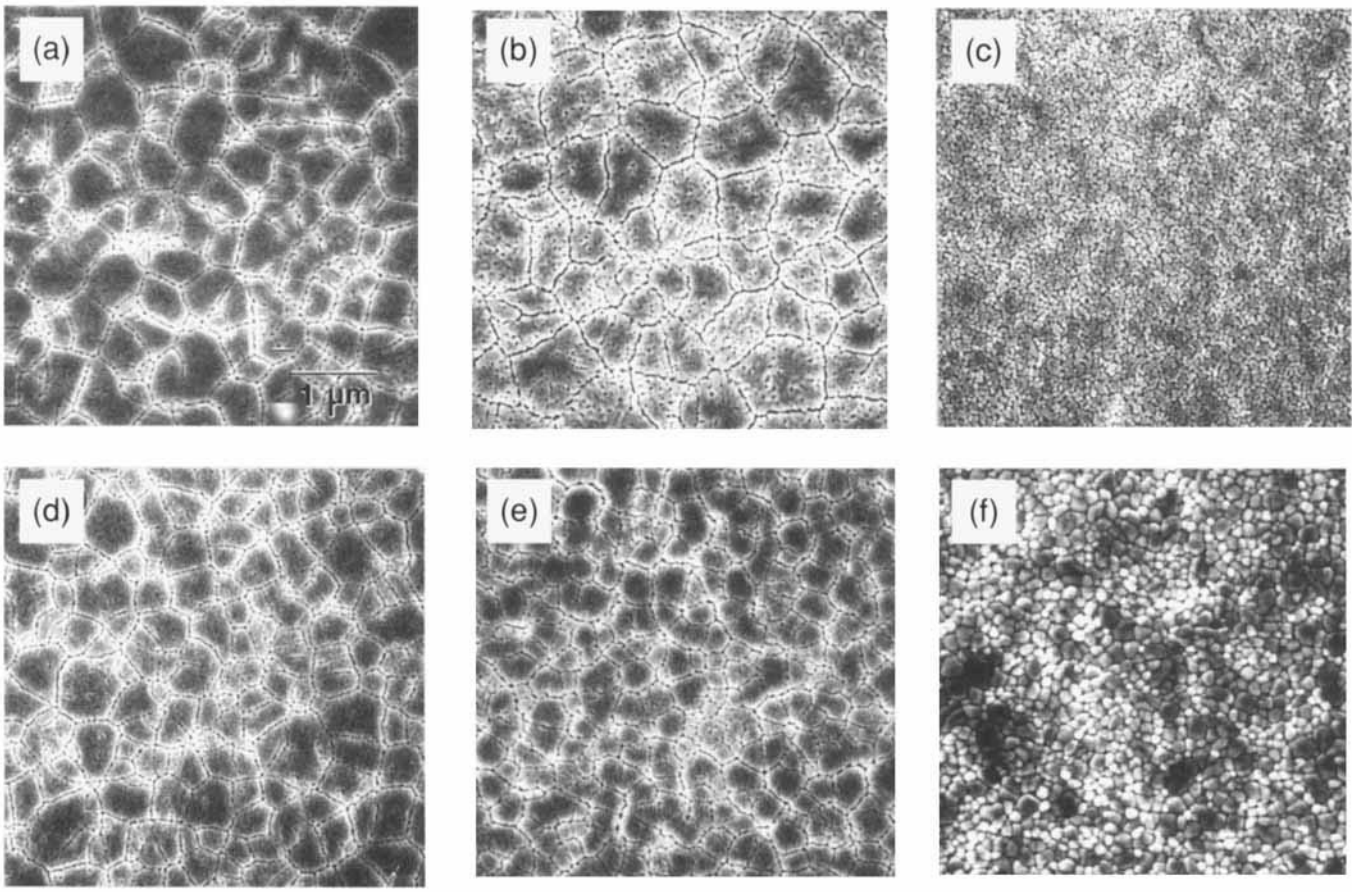

Fig. 11. SEM micrographs of $Pb(Zr_{1-x}Ti_x)O_3$ films for (a) $x = 0.25$, (b) $x = 0.48$, and (c) $x = 0.75$ pyrolyzed at 450°C (0.5 h) and annealed at 700°C, and for (d) $x = 0.25$, (e) $x = 0.48$, and (f) $x = 0.75$ rapidly heated to 700°C.

IV. Conclusions

(1) The heat treatment conditions, in terms of annealing temperature, annealing time, and heating rate, for obtaining $Pb(Zr_{1-x}Ti_x)O_3$ films with [111] and [100] textures have been determined. Intermediate phases preceding the formation of textured PZT films are identified.

(2) The formation of textured PZT is controlled by the nucleation step during which either $Pt_{5-7}Pb$ or PbO forms, leading to [111] or [100] texture that can be further developed by subsequent growth. A TTT diagram delineating the nucleation conditions for these textures is presented to aid design of heat treatment schedules.

(3) The Pb composition is important for [100] texture because Pb excess facilitates PbO formation. The Zr/Ti ratio has a secondary effect on [100] texture due to the compositional effect on PbO activity.

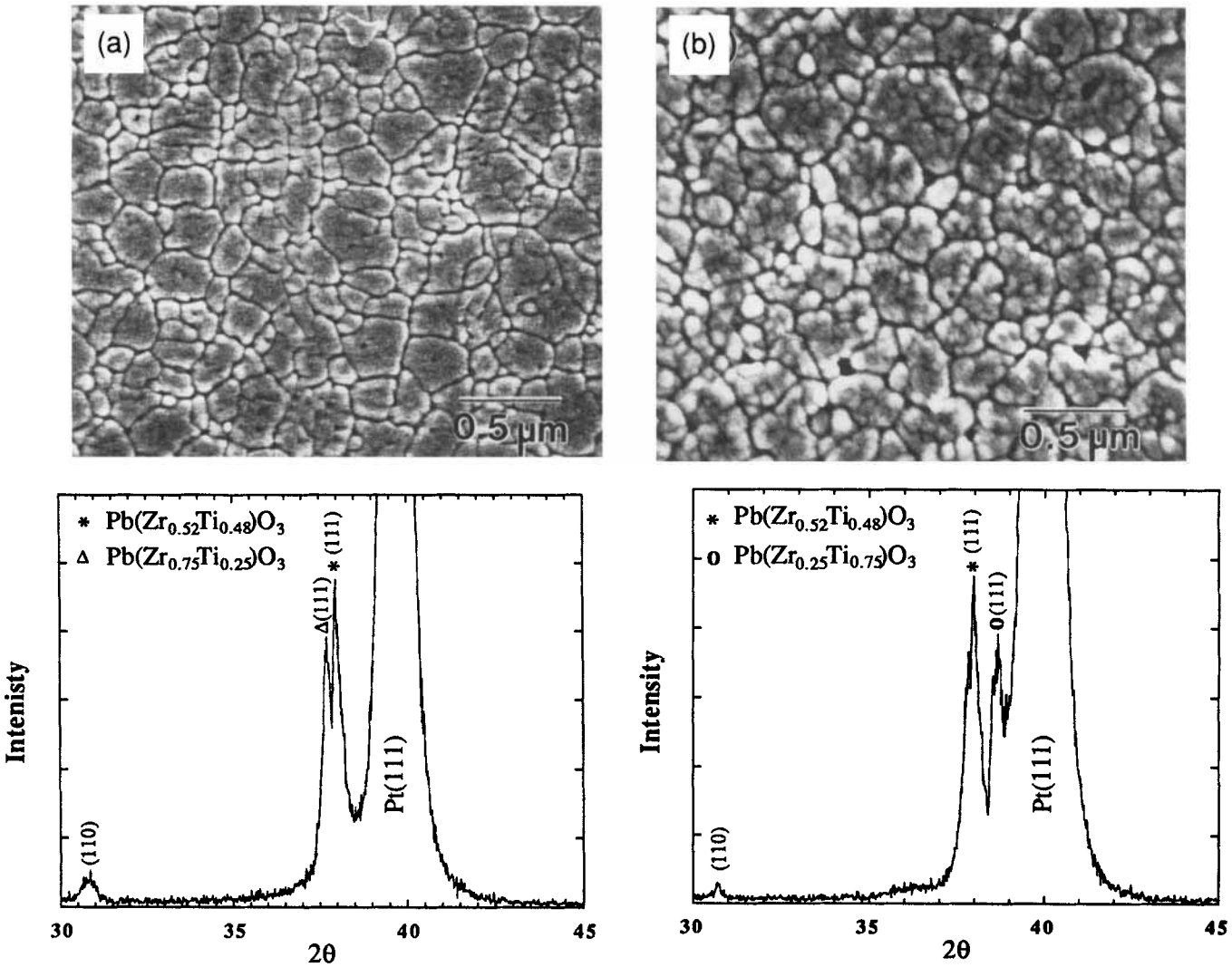

Fig. 12. SEM micrographs and XRD patterns of (a) $Pb(Zr_{0.75}Ti_{0.25})O_3$ and (b) $Pb(Zr_{0.25}Ti_{0.75})O_3$ films grown on a first layer of $Pb(Zr_{0.52}Ti_{0.48})O_3(111)$. The heat treatment used was fast heating to 700°C for both the first and the outer layers.

(4) For [111] texture, only Zr/Ti ratio is important due to the consideration of lattice matching which is poor for Zr-rich compositions.

(5) Microstructure and texture of PZT films can be manipulated by controlling the seeding step utilizing relations governing texture and crystallization.

References

[1]V. E. Wood, J. R. Busch, S. D. Ramamurthi, and S. L. Swartz, "Guided-Wave Optical Properties of Sol–Gel Ferroelectric Films," *J. Appl. Phys.*, **72** [9] 4557–66 (1992).

[2]S. Hirano, T. Yogo, K. Kikuta, Y. Araki, M. Saitoh, and S. Ogasahara, "Synthesis of Highly Oriented Lead Zirconate–Lead Titanate Film Using Metallo-Organics," *J. Am. Ceram. Soc.*, **75** [10] 2785–89 (1992).

[3]G. Teowee, J. M. Boulton, S. C. Lee, and D. R. Uhlmann, "Electrical Characterization of Sol–Gel Derived PZT Films," *Mater. Res. Soc. Symp. Proc.*, **243**, 255–61 (1992).

[4]B. A. Tuttle, J. A. Voigt, D. C. Goodnow, D. L. Lamppa, T. J. Headley, M. O. Eatough, G. Zender, R. D. Nasby, and S. M. Rodgers, "Highly Oriented, Chemically Prepared $Pb(Zr,Ti)O_3$ Thin Films," *J. Am. Ceram. Soc.*, **76** [6] 1537–44 (1993).

[5]T. Tani, Z. Xu, and D. A. Payne, "Preferred Orientations for Sol–Gel Derived PLZT Thin Layers," *Mater. Res. Soc. Symp. Proc.*, **310**, 269–74 (1993).

[6]M. Klee, R. Eusemann, R. Waser, and W. Brand, "Processing and Electrical Properties of $Pb(Zr_xTi_{1-x})O_3$ (x = 0.2–0.75) Films: Comparison of Metallo-Organic Decomposition and Sol–Gel Processes," *J. Appl. Phys.*, **72** [4] 1566–76 (1992).

[7]S. Y. Chen and I-W. Chen, "Phase Transformations of Orientation $Pb(Zr_{1-x}Ti_x)O_3$ Thin Films from Metallo-Organic Precursors," *Ferroelectrics*, **152** [124] 25–30 (1994).

[8]S. Y. Chen and I-W. Chen, "Temperature–Time Texture Transition of $Pb(Zr,Ti)O_3$ Thin Films: I, The Role of Pb-rich Intermediate Phases," *J. Am. Ceram. Soc.*, **77** [9] 2332–36 (1994).

[9]R. W. Vest, "Electronic Films from Metallo-Organic Precursors"; pp. 303–41 in *Ceramic Films and Coating*. Edited by J. B. Wachtman and R. A. Haber. Noyes Publications, Park Ridge, NJ, 1993.

[10]C. D. E. Lukeman, J. Campion, and D. A. Payne, "Factors Affecting the Sol–Gel Processing of PZT Thin Layers"; pp. 413–39 in Ceramic Transactions, Vol. 25, *Ferroelectric Films*. Edited by A. S. Bhalla and K. M. Nair. American Ceramic Society, Westerville, OH, 1992.

[11]G. W. Scherer and T. J. Garono, "Viscous Sintering on a Rigid Substrate," *J. Am. Ceram. Soc.*, **68** [4] 216–20 (1985).

[12]B. A. Tuttle, R. W. Schwartz, D. H. Doughty, and J. A. Voigt, "Characterization of Chemically Prepared PZT Thin Films," *Mater. Res. Soc. Symp. Proc.*, **200**, 59–65 (1990).

[13]G. R. Fox, S. B. Krupanidhi, and K. L. More, "Composition/Structure/Property Relations of Multi-Ion-Beam Reactive Sputtered Lead Lanthanum Titanate Thin Films: Part I. Composition and Structure Analysis," *J. Mater. Res.*, **7** [11] 3039–55 (1992).

[14]D. A. Porter and K. E. Easterling, *Diffusional Transformations in Solids, Phase Transformations in Metals and Alloys*; Ch. 5. van Nostrand Reinhold, New York, 1981.

[15]K. Iijima, Y. Tomita, R. Takayama, and I. Ueda, "Preparation of c-axis Oriented $PbTiO_3$ Thin Films and Their Crystallographic, Dielectric, and Pyroelectric Properties," *J. Appl. Phys.*, **60** [1] 361–67 (1986).

[16]R. Takayama and Y. Tomita, "Preparation of Epitaxial $Pb(Zr,Ti_{1-x})O_3$ Thin Films and Their Crystallographic, Pyroelectric and Ferroelectric Properties," *J. Appl. Phys.*, **65** [4] 1666–70 (1989).

[17]D. Xiao, J. Zhu, J. Zhu, Z. Xiao, Z. Qian, and H. Zhang, "The Orientation of $(Pb,La)TiO_3$ Thin Films Grown on Different Substrates by Multi-Ion-Beam Reactive Cosputtering Technique," *Ferroelectrics*, **141**, 327–33 (1993).

[18]R. L. Holman and R. M. Fulrath, "Intrinsic Nonstoichiometry in the Lead-Zirconate-Lead Titanate System Determined by Knudsen Effusion," *J. Appl. Phys.*, **44** [12] 5227–36 (1973). □